Covalent gold

Lai-Sheng Wang

Received 4th March 2010, Accepted 30th April 2010
DOI: 10.1039/c003886e

Gold is known to be the noblest of all metals because of the relativistic stabilization of its outer 6s orbital. The relativistic effects also lead to destabilization of the 5d orbitals, reducing the 6s-5d energy gap and enhancing s-d hybridization. Therefore, in contrast to its lighter congeners, gold exhibits significant covalent bonding characters and a remarkable repertoire of chemistry, which are increasingly being exploited in catalysis and nanotechnology. This Perspective presents a brief account of recent experimental efforts in the author's laboratory using photoelectron spectroscopy that lead to direct observations of covalent bonding in several relatively simple Au compounds: Au oxides (AuO^- and AuO_2^-), sulfides (AuS^- and AuS_2^-), and the well-known $Au(CN)_2^-$ complex. In a series of Au–Si and Au–B mixed clusters, it has also been found that gold atoms behave like H atoms, forming auro-silicon and auro-boron clusters with strong covalent bonding, analogous to the corresponding silicon and boron hydrides, such as the tetrahedral auro-silane ($SiAu_4$) *versus* silane (SiH_4).

1. Introduction

Gold possesses a valence electron configuration of $5d^{10}6s^1$ with a filled 5d shell and a 6s shell similar to the alkali atoms. However, gold displays a "relativistic maximum"[1] that results in some unusual physical and chemical properties for the noblest of all metals. The relativistic effects significantly stabilize the 6s orbital, resulting in an anomalously high ionization potential (9.225 eV) and an extremely high electron affinity (2.309 eV) for the gold atom. On the Pauling scale, the electronegativity of gold, the highest among the metallic elements, is 2.4, which is the same as Se and close to that of S (2.5) and I (2.5). Thus, even ionic compounds, in which gold acts as an *electron acceptor*, are known, such as in CsAu (Cs^+Au^-). The relativistic effects also destabilize the 5d orbitals, leading to a reduction of the s-d energy gap, and thus endow gold with its enchanting color, which has fascinated humankind since the ancient. Hence, despite the fact that gold is known to be the noblest of all metals, it exhibits strong covalent bonding characters due to s-d hybridization and displays a remarkable repertoire of chemistry.

The chemistry of gold is undergoing a renaissance because of the increasingly important roles gold plays in catalysis and nanotechnology. The covalent bonding nature of gold is at the core of ligand-protected gold nanoparticles and homogeneous catalyses of organogold. Numerous reviews have appeared on various aspects of gold chemistry.[2–5] The extensive theoretical and experimental literature on gold up to 2007 has been summarized comprehensively by Pyykkö in a trilogy of reviews.[6–8] The relativistic effects in gas-phase ion chemistry were reviewed by Schwarz.[9] The interactions between thiolate ligands and gold are critical to self-assembled monolayers and ligand-protected gold nanoparticles. Both experimental and theoretical studies have shown that the ligands adsorb on atop positions with significant covalent bonding between the thiolate and the substrate.[10–14] Even the highly electronegative Cl atoms on Au surfaces have been found to exhibit significant covalent bonding with the substrate.[15] In the past decade, homogeneous Au catalysis for efficient and selective activation of C–C π bonds has undergone rapid development and has been widely reviewed.[4,5] The nature of the Au–C bond has received particular attention.[16–20] The discovery of heterogeneous catalysis by supported gold nanoparticles[21] has stimulated a flurry of activities both in catalysis and in cluster science to elucidate the nature of the catalytic mechanisms.[3,22,23] Novel structures of gold clusters, as a result of the s-d hybridization, have been observed.[24–27]

This Perspective focuses on recent experimental efforts in the author's laboratory using photoelectron spectroscopy

Department of Chemistry, Brown University, Providence, RI 02912, USA. E-mail: Lai-Sheng_Wang@brown.edu

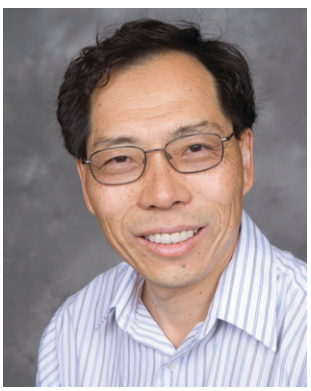

Lai-Sheng Wang

Lai-Sheng Wang received his PhD from the University of California at Berkeley. After a postdoctoral stay at Rice University, he took a joint position between Washington State University and Pacific Northwest National Laboratory in 1993, then moved to Brown University as Professor of Chemistry in 2009. His research focuses on the investigation of the fundamental behaviors of nanoclusters using photoelectron spectroscopy. Research in his group has led to the discovery of golden buckyballs and golden pyramids, as well as aromatic clusters and planar boron clusters. His group has also pioneered spectroscopic studies in the gas-phase of free multiply-charged anions and complex solution-phase anions, such as metal complexes, redox species, and biologically-relevant molecules.

 This journal is © the Owner Societies 2010

(PES) to investigate the electronic structures and chemical bonding of several relatively simple Au-containing molecules and binary Au alloy clusters, in which significant covalent bond characters of Au have been observed. Specifically, three classes of species will be discussed: (i) gold oxides (AuO^- and AuO_2^-) and sulfides (AuS^- and AuS_2^-); (ii) gold as hydrogen in Au–Si and Au–B binary clusters; and (iii) $Au(CN)_2^-$. PES involves electron removals from valence molecular orbitals and provides direct information about the nature of the chemical bonding. The covalent nature of the Au–O and Au–CN bonding is directly revealed in the PES spectra. In conjunction with theoretical calculations, the structures and chemical bonding can be investigated in great detail. In a series of Au–Si and Au–B clusters, we have found that Au behaves like H, forming strong auride covalent bonds and yielding cluster structures analogous to the corresponding hydrides.

2. Covalent bonding in Au oxide and sulfide molecules

The Au–O and Au–S interactions are essential in nanogold catalysis and ligand-protected gold nanoparticles, for which mono-gold oxide and sulfide clusters can serve as the simplest molecular models. However, except for a few theoretical and spectroscopic studies on the diatomic AuO,[28–32] there was limited knowledge about the AuO_2 or the sulfide systems.[33] Although there were early matrix studies on the Au–O_2 complex,[34–38] we now know that Au or Au^- can only form weakly bound van der Waals complexes with O_2 or the linear dioxide molecules via the reaction of $AuO + O$.[39,40] A combined PES and *ab initio* study on AuO^- and AuO_2^- and their valent isoelectronic AuS^- and AuS_2^- species was carried out to probe their electronic structure and to elucidate the Au–O and Au–S chemical bonding.[41] Vibrationally-resolved PES spectra were obtained at different photon energies, providing a wealth of electronic structure information for each species. Similar spectra were observed for AuO^- and AuS^- and for the linear $OAuO^-$ and $SAuS^-$ species. High-level *ab initio* calculations (Table 1) were conducted to aid spectral assignments and provide insight into the chemical bonding in the AuX^- and AuX_2^- (X = O, S) molecules. Configuration interactions and spin–orbit couplings were shown to be important and were necessary to achieve good agreement between theory and experiment. Strong covalent bonding was found in both the AuX^- and the $XAuX^-$ species with multiple bonding characters.

2.1 Multiple bonding in AuO^- and AuS^-

Fig. 1 shows the vibrationally-resolved PES spectra of AuO^- at three different detachment photon energies.[41] The spectra of AuS^- are similar to those of AuO^-. The high photon energy spectrum at 193 nm revealed electron detachments from 5d-based molecular orbitals (MOs) and was important in elucidating the nature of the Au–O bonding. Fig. 2 displays the MO diagram for AuO^- and AuS^- and Fig. 3 shows the MO pictures for AuO^-. The O $p_{x/y}$ orbitals and Au $5d_{xz/yz}$ orbitals form the bonding π (HOMO-3) and antibonding π* HOMO, which are both fully occupied in the anionic ground state. The O p_z orbital interacts with the Au 6s and $5d_{z^2}$ orbitals to form the bonding 1σ (HOMO-4), non-bonding 2σ (HOMO-1) and the unoccupied antibonding σ* LUMO, whereas the δ MO (HOMO-2) is purely nonbonding. The X and A bands in Fig. 1 correspond to electron detachments from the O2p-based π* and 2σ MOs, respectively, and the B band corresponds to electron detachment from the δ MO. The C/D and E bands derive from detachments from the Au5d-based π and 1σ MOs, respectively. The extensive vibrational structures associated with these bands provide direct spectroscopic evidence that the 1σ and π MOs are strongly bonding orbitals. On the other hand, the PES spectra for CuO^- display no such vibrational activities for detachments from similar MOs because they are non-bonding.[42]

Table 1 Summary of the ground state properties obtained at the CCSD(T) level of theory for $AuX_{1,2}^-$ (X = O, S) and the measured electron affinities (EA) for the corresponding neutral molecules. All energies are given in eV and bond lengths (r_{Au-X}) are in Å

		State	r_{Au-X}	$D_e(X)^a$	EA
AuO^-	$C_{\infty v}$	$^1\Sigma^+$	1.882	2.082	2.378 ± 0.015
$OAuO^-$	$D_{\infty h}$	$^3\Sigma_g^-$	1.847	4.046	3.40 ± 0.03
AuS^-	$C_{\infty v}$	$^1\Sigma^+$	2.216	2.677	2.475 ± 0.015
$SAuS^-$	$D_{\infty h}$	$^3\Sigma_g^-$	2.202	3.388	3.42 ± 0.03

[a] Dissociation energy for the most stable fragments regardless of spin, defined as:. $E(AuX_n^-) - [E(AuX_{n-1}^-) + E(X)]$ with n = 1, 2 and X = O, S.

The nonbonding nature of the 2σ and δ MOs in AuO^- is confirmed by the PES spectra in Fig. 1, which show very little Franck–Condon activity upon electron removals from these MOs. Thus, on the basis of the MO configuration (Fig. 2), the AuX^- molecules possess a single σ bond derived from the 1σ bonding MO because the bonding 1π and the antibonding π* MOs cancel each other. However, while the strong bonding nature of the 1σ and 1π MOs are confirmed by the PES spectra (strong Franck–Condon activities), the π* HOMO is somewhat nonbonding as evidenced by the very weak Franck–Condon activities in the spin–orbit split X bands (Fig. 1a). Thus, the AuX^-species contain some π bonding character. If the π* HOMO were completely nonbonding, the bond in AuX^- could be characterized as a triple bond. Indeed, the calculated bond lengths of AuX^- (Table 1) are only slightly smaller than the sums of the Au and X triple bond covalent radii proposed by Pyykkö *et al.* (1.76 Å for AuO and 2.18 Å for AuS).[43] Since the π* HOMO does have some antibonding character, the chemical bond in AuX^- is less than a triple bond. Removing the four π* electrons would lead to a real triply bonded AuX diatomic species, which corresponds to the electron configuration of AuC^+ or $AuSi^+$. Indeed, these species have been predicted previously as containing a triple bond.[44]

2.2 Covalent bonding in AuO_2^- and AuS_2^-

The Au^- atomic anion does not react with O_2 and they can only form a weakly bonded van der Waals complex, $Au^-(O_2)$, which has been recently reported.[39,40] On the other hand, Au^- forms a relatively strongly bonded $Au^-(S_2)$ complex with a substantial binding energy (1.4 eV), which was observed in our laser vaporization cluster source as a minor isomer.[41]

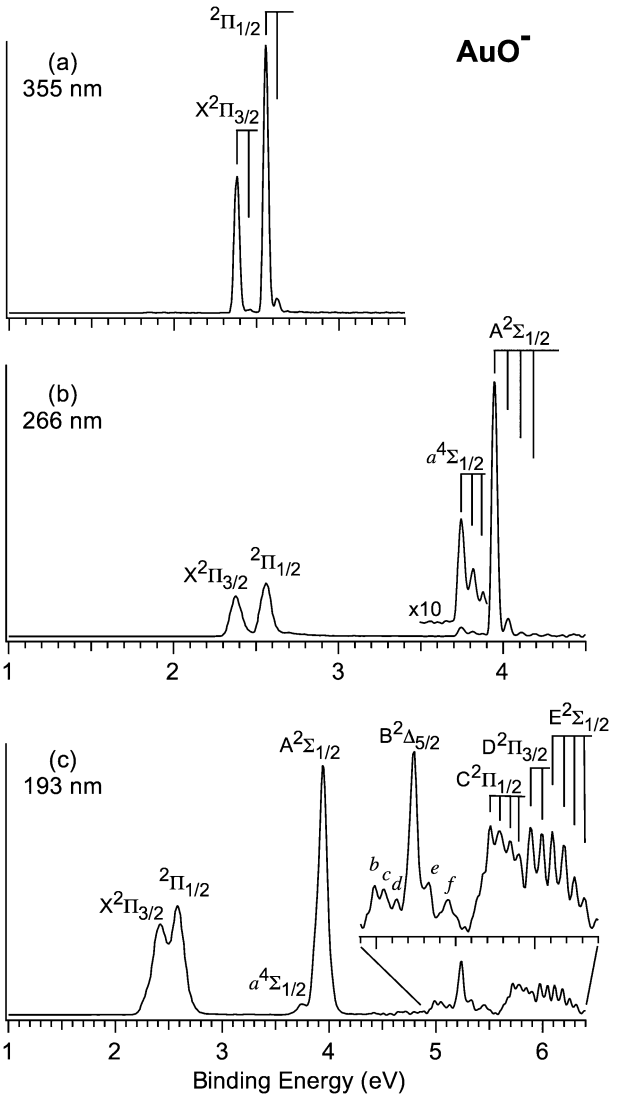

Fig. 1 Photoelectron spectra of AuO^- at (a) 355 nm (3.496 eV), (b) 266 nm (4.661 eV), and (c) 193 nm (6.424 eV). The vertical lines represent the resolved vibrational structures. The detailed assignments are given in ref. 41.

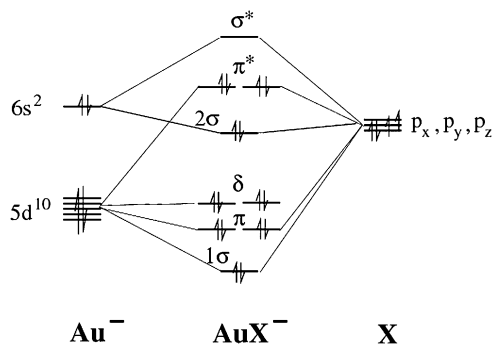

Fig. 2 Molecular orbital diagram for AuO^- and AuS^-.

However, Au can form stable linear dioxide and disulfide molecules ($XAuX^-$) by reactions of AuX^- with the atomic species (X). Vibrationally resolved PES spectra at different photon energies were obtained for AuX_2^- and their structures

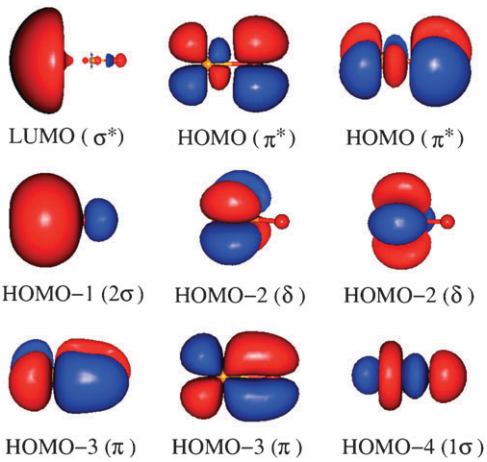

Fig. 3 Molecular orbital pictures for AuO^-.

and chemical bonding were analyzed by comparing with *ab initio* calculations.

Fig. 4 shows the MO diagram of AuO_2^- and AuS_2^-; and Fig. 5 displays the MO pictures of AuO_2^-. The bonding in $SAuS^-$ is very similar to that in $OAuO^-$ with nearly identical MO pictures. The O(S) $p_{x/y}$ orbitals interact with the Au($5d_{yz}$,$5d_{xz}$) orbitals to form the strongly bonding $1\pi_g$ HOMO-5, the non-bonding $1\pi_u$ HOMO-1, and the antibonding $2\pi_g$ HOMO. The $2\pi_g$ HOMO is half-occupied, resulting in the triplet ground state for AuX_2^- ($^3\Sigma_g^-$, Table 1). The interactions of O(S) p_z with Au 6s and $5d_{z^2}$ yield the strong bonding $1\sigma_g$, the bonding $2\sigma_g$, the weakly bonding $1\sigma_u$, and the antibonding σ_g* LUMO. The antibonding character of the $2\pi_g$ HOMO was confirmed by observation of substantial Franck–Condon activities in the PES spectra of AuX_2^- and the increased Au–X stretching vibrational frequency in the neutrals compared to the anions. The $1\pi_u$, $2\sigma_g$, and $1\sigma_u$ MOs are basically nonbonding according to the PES spectra since there is very little Franck–Condon activity upon electron removals from these orbitals. Thus, the Au–X bonding in AuX_2^- should also have substantial multiple bonding characters.

Interestingly, the Au–X bond is significantly strengthened in AuX_2^- compared to that in the AuX^- diatomics, as seen in Table 1. In particular, the dissociation energy of 4.046 eV for $AuO_2^- \rightarrow AuO^- + O$ is almost twice as large as the AuO^- dissociation energy (2.082 eV for $AuO^- \rightarrow Au^- + O$). This enhanced Au–X bonding in AuX_2^- is also reflected in their shortened Au–X distances (Table 1). The enhanced Au–X bonding in AuX_2^- is most likely due to the partially occupied $2\pi_g$ antibonding orbitals, as well as from the strong covalent bonding interactions between the Au 5d and O(S) p atomic orbitals embodied in the $1\sigma_g$ and $1\pi_g$ MOs (Fig. 5). Overall, the Au–O and Au–S bonds in the AuX^- and AuX_2^- molecules are strongly covalent with multiple bond characters due to the s–d hybridization.

3. Au as H in Au–Si and Au–B alloy clusters

The isolobal analogy between a gold phosphine unit ($AuPR_3$) and a hydrogen atom have been well recognized in

This journal is © the Owner Societies 2010

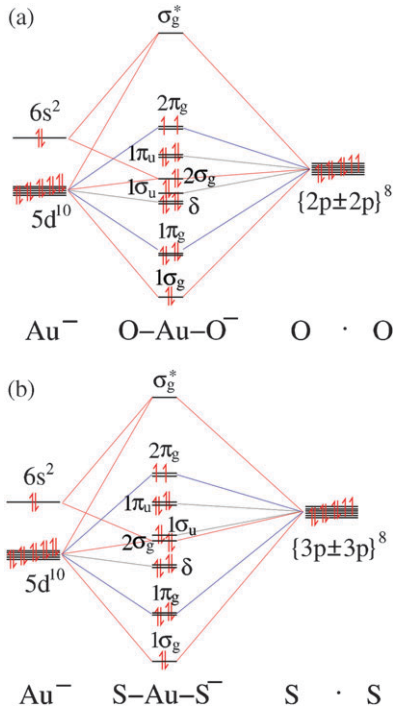

Fig. 4 Molecular orbital diagram for AuO_2^- and AuS_2^-.

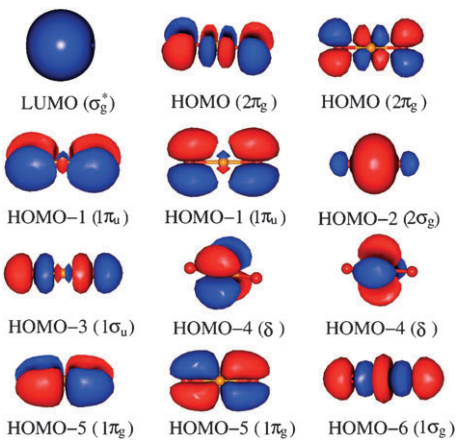

Fig. 5 Molecular orbital pictures for AuO_2^-.

organometallic chemistry,[45–47] such as in the tetra- and hypercoordinate compounds, $C(AuPR_3)_4$ and $C(AuPR_3)_5^+$.[48,49] The Au^+ cation has been found to act like a "big proton" in a number of gas phase ion-molecule complexes.[9] In a PES study of mono-silicon gold alloy clusters ($SiAu_n^-$, n = 2–4),[50] we found serendipitously that the Au atoms behave like H atoms in the mixed clusters, resulting in structures analogous to silicon hydrides (SiH_n, n = 2–4). The silicon tetraauride ($SiAu_4$), which was considered in a prior computational study,[51] is found to be particularly stable with a large HOMO–LUMO gap similar to silane SiH_4. Molecular orbital analyses showed that Si and Au form strong single covalent bonds in these clusters with bonding energies very close to the corresponding Si–H bonds. Both PES and theoretical studies revealed that larger Si–Au alloy clusters are also similar to the corresponding silicon hydrides. It was further found that Au and boron form binary clusters, in which Au also behaves like H. Based on this finding, a series of deltahedral closo-auroboranes ($B_nAu_n^{2-}$, n = 5–12) in analogy to the well-known deltahedral closoboranes ($B_nH_n^{2-}$) have been predicted, which may be viable for chemical syntheses.

3.1 $SiAu_n^-$ and $SiAu_n$ (n = 2–4)

The PES spectra of $SiAu_n^-$ (n = 2–4) are given in Fig. 6 at two detachment photon energies.[50] The most interesting observation was the extremely large energy gap between the X and A bands observed in the spectra of $SiAu_4^-$ (Fig. 6e and f), suggesting a highly stable neutral $SiAu_4$ species with a large HOMO–LUMO gap. The ground state transition of $SiAu_4^-$ was vibrationally resolved, consisting of a single vibrational progression with a spacing of 140 ± 30 cm^{-1} (inset, Fig. 6f). This observation indicated that the $SiAu_4^-$ anion and $SiAu_4$ neutral must possess relatively high symmetries. Theoretical calculations showed that the most stable structures of $SiAu_4^-$ and $SiAu_4$ are both tetrahedral, as shown in Fig. 7e. The simulated PES spectrum of the tetrahedral $SiAu_4^-$ agrees well with the experimental spectra, lending strong support for the global minimum structures found for the $SiAu_4^-$ anion and its neutral. The tetrahedral structure, in which there is no Au–Au bonding, is much more stable than the square-pyramidal structure (Fig. 7f). Further calculations showed that the most stable structures of $SiAu_3^-$ and $SiAu_2^-$ and their neutrals are C_{3v} and C_{2v}, respectively, which can be viewed simply as removing one and two Au atoms from the T_d $SiAu_4^-$ (Fig. 7a and c), respectively.

Remarkably, the global minimum structures of the mono-silicon aurides, $SiAu_n$ (n = 2–4), are all similar to those of the silicon hydrides, SiH_n (n = 2–4). As shown in Fig. 8, MO analyses revealed that the chemical bonding in $SiAu_n$ are also similar to the corresponding SiH_n molecules, suggesting that Au behaves like a H in the auride clusters by forming a single Si–Au covalent bond. To evaluate the stability of the new silicon auride molecules, their atomization energies [at CCSD(T) level] were calculated and compared to the corresponding silicon hydrides:[50]

$$SiAu_2\ (C_{2v},\ ^1A_1) \rightarrow Si\ (^3P) + 2Au\ (^2S)\ \Delta E = 5.82\ eV\ (134.2\ kcal/mol)$$

$$SiH_2\ (C_{2v},\ ^1A_1) \rightarrow Si\ (^3P) + 2H\ (^2S)\ \Delta E = 6.52\ eV\ (150.4\ kcal/mol)$$

$$SiAu_3\ (C_{3v},\ ^2A_1) \rightarrow Si\ (^3P) + 3Au\ (^2S)\ \Delta E = 7.89\ eV\ (181.9\ kcal/mol)$$

$$SiH_3\ (C_{3v},\ ^2A_1) \rightarrow Si\ (^3P) + 3H\ (^2S)\ \Delta E = 9.68\ eV\ (223.2\ kcal/mol)$$

$$SiAu_4\ (T_d,\ ^1A_1) \rightarrow Si\ (^3P) + 4Au\ (^2S)\ \Delta E = 10.87\ eV\ (250.7\ kcal/mol)$$

$$SiH_4\ (T_d,\ ^1A_1) \rightarrow Si\ (^3P) + 4H\ (^2S)\ \Delta E = 13.80\ eV\ (318.2\ kcal/mol)$$

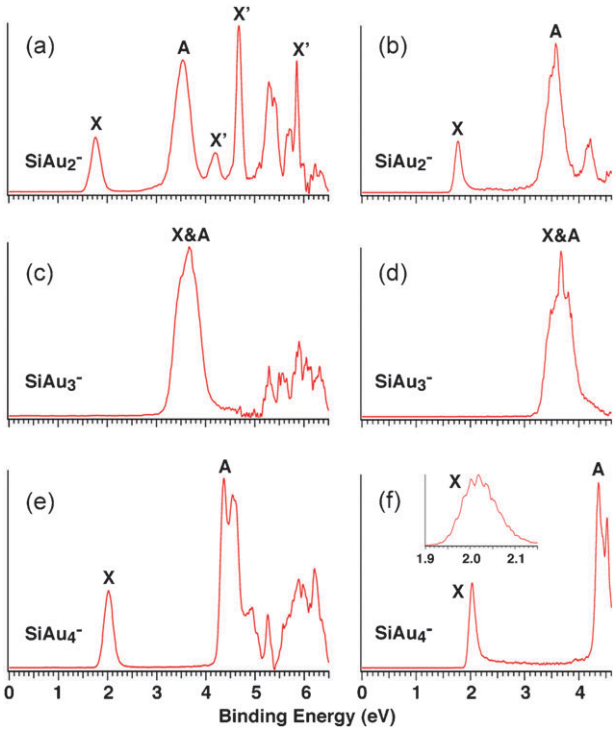

Fig. 6 Photoelectron Spectra of $SiAu_n^-$ (n = 2–4). (a) $SiAu_2^-$ at 193 nm. (b) $SiAu_2^-$ at 266 nm. (c) $SiAu_3^-$ at 193 nm. (d) $SiAu_3^-$ at 266 nm. (e) $SiAu_4^-$ at 193 nm. (f) $SiAu_4^-$ at 266 nm; the inset shows the spectrum of $SiAu_4^-$ taken at 532 nm (2.331 eV).

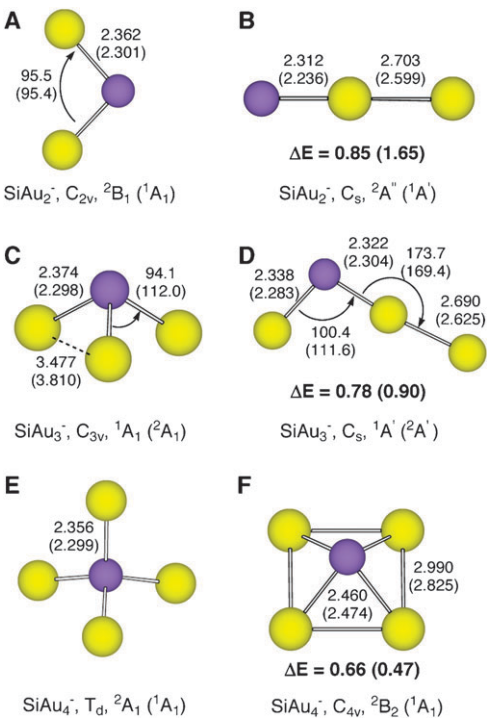

Fig. 7 Optimized structures for the global minimum and low-lying isomers of $SiAu_n^-$ and $SiAu_n$. All bond lengths are given in angstroms and angles in degrees. The relative energies (in bold) are in eV for the higher energy isomer. The values in the parentheses correspond to the neutral structures. See ref. 50 for computational details.

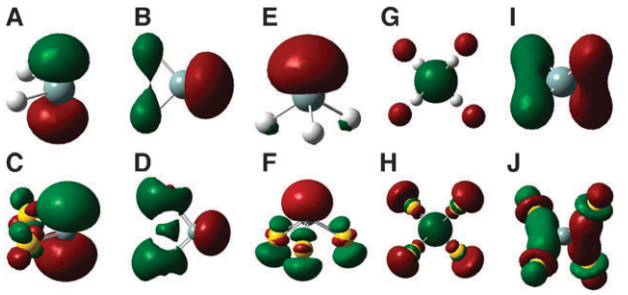

Fig. 8 Comparison of the relevant frontier molecular orbitals between SiH_n and $SiAu_n$ (n = 2–4). (A) The LUMO (b_1) of SiH_2. (B) The HOMO (a_1) of SiH_2. (C) The LUMO (b_1) of $SiAu_2$. (D) The HOMO (a_1) of $SiAu_2$. (E) The HOMO (a_1) of SiH_3. (F) The HOMO (a_1) of $SiAu_3$. (G) The LUMO (a_1) of SiH_4. (H) The LUMO (a_1) of $SiAu_4$. (I) one of the three Si–H bonding orbitals of SiH_4 (t_2). (J) one of the three Si–Au bonding orbitals of $SiAu_4$ (t_2).

The total atomization energies, as well as the single Si–Au bond energies in $SiAu_2$ (67.1 kcal/mol), $SiAu_3$ (60.6 kcal/mol), and $SiAu_4$ (62.7 kcal/mol), are quite high and they are

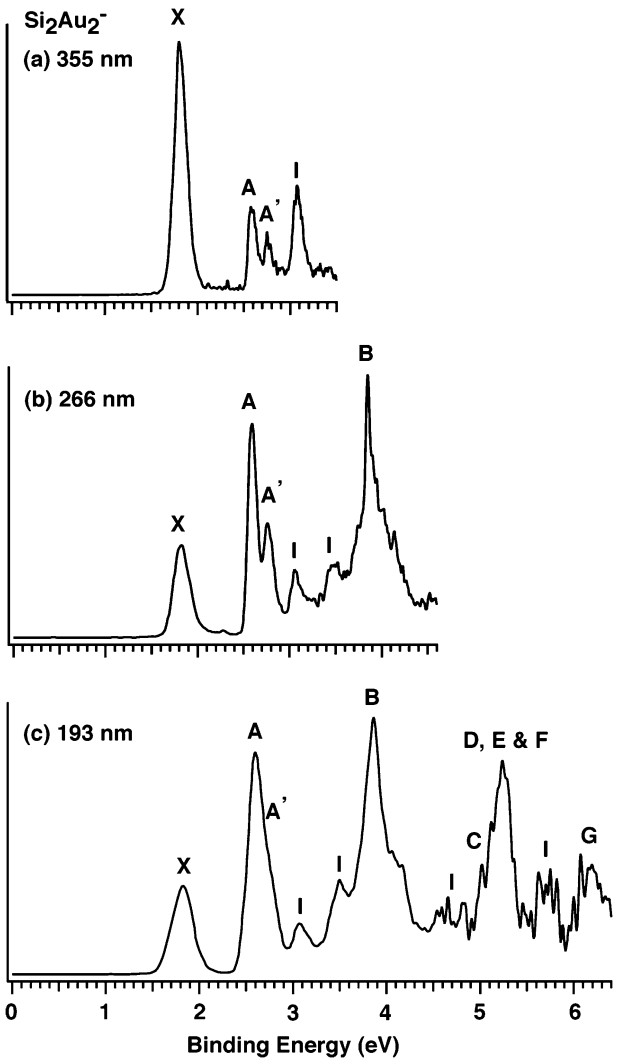

Fig. 9 Photoelectron spectra of $Si_2Au_2^-$ at (a) 355 nm, (b) 266 nm, and (c) 193 nm.

This journal is © the Owner Societies 2010

close to those in the corresponding Si–H molecules, SiH_2 (75.2 kcal/mol), SiH_3 (74.4 kcal/mol), and SiH_4 (79.6 kcal/mol).[52] These relatively high atomization energies and strong Si–Au bonds reflect both the covalent nature of the Si–Au bonds and the high stability of the $SiAu_n$ silicon auride molecules.

3.2 $Si_2Au_n^-$ and Si_2Au_n (n = 2 and 4), and $Si_3Au_3^+$, Si_3Au_3, and $Si_3Au_3^-$

To test the generality of the Au–H analogy, several larger Si–Au binary clusters have been produced and investigated.[53,54] Fig. 9 and 10 display the PES spectra of $Si_2Au_2^-$ and $Si_2Au_4^-$ at various photon energies, which were used to compare with theoretical calculations to determine the most stable structures of $Si_2Au_n^-$ and Si_2Au_n (n = 2 and 4).[53] It is well known that the acetylene and ethylene analogues of silicon do not possess the classical configurations. Instead, they prefer to form hydrogen-bridged or other distorted nonclassical structures.[55–58] We found that the di-silicon aurides also prefer nonclassical structures analogous to the corresponding hydrides. Similar to Si_2H_2, the most stable structure for Si_2Au_2 has a dibridged configuration. For Si_2Au_4, the most stable isomer corresponds to a mono-bridged structure. More interestingly, we found that the potential energy surfaces of the di-silicon-gold systems are also very similar to those of the corresponding hydrides with similar low-lying isomeric structures. In Fig. 11, the MOs of Si_2Au_2 and Si_2Au_4 are compared to their hydride counterparts. The similarity in both structure and bonding between the aurides and hydrides of the di-silicon systems are clearly shown.

We have also measured the PES of $Si_3Au_3^-$ and investigated the Au–H analogy in the tri-silicon gold clusters.[54] PES and density functional calculations were combined to examine the geometric and electronic structure of $Si_3Au_3^-$. It was found that there are three isomers competing for the ground state of $Si_3Au_3^-$, as is the case for $Si_3H_3^-$.[59] Extensive structural searches showed that the potential energy surfaces of the tri-silicon gold clusters ($Si_3Au_3^-$, Si_3Au_3, and $Si_3Au_3^+$) are similar to those of the corresponding silicon hydrides. The lowest energy isomers for $Si_3Au_3^-$ and Si_3Au_3 are structurally similar with a Si_3Au four-membered ring serving as a common structural motif. The $Si_3Au_3^+$ cation is interesting because its hydride analog, the cyclotrisilenylium ion (D_{3h} $Si_3H_3^+$) is a 2π aromatic species, which has been extensively studied.[60–64] An aromatic cyclotrisilenylium ion with bulky substituents,

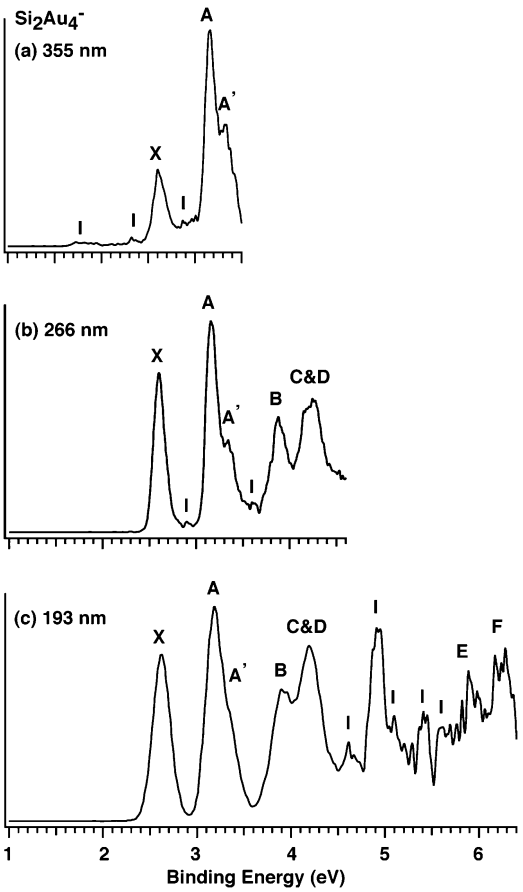

Fig. 10 Photoelectron spectra of $Si_2Au_4^-$ at (a) 355 nm, (b) 266 nm, and (c) 193 nm.

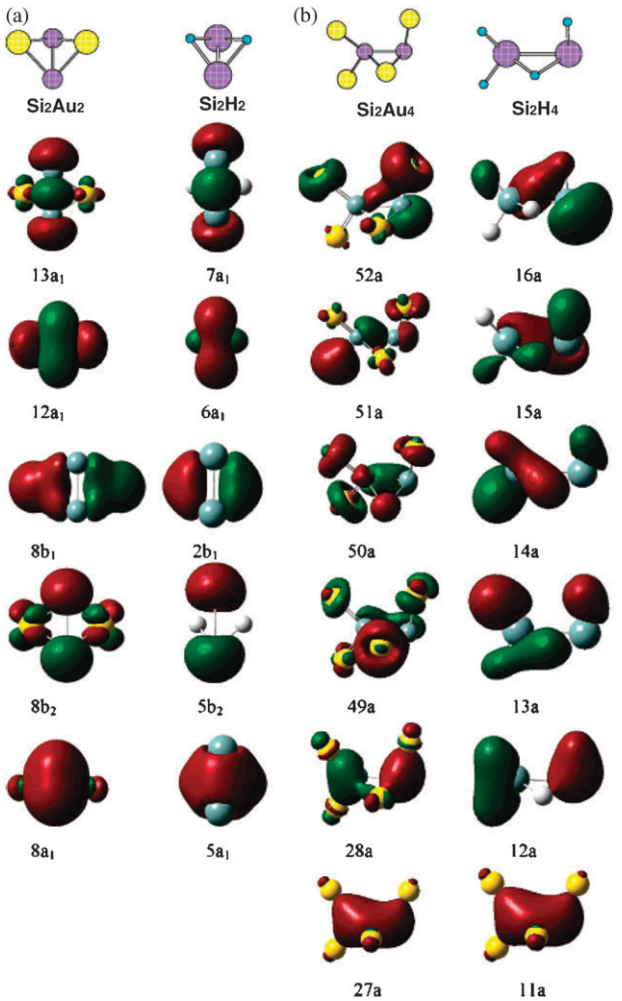

Fig. 11 (a) Comparisons of the five bonding molecular orbitals of the global minimum dibridged structure of Si_2Au_2 with the corresponding structure and molecular orbitals of Si_2H_2. (b) Comparison of the six bonding molecular orbital pictures of the global minimum mono-bridged structure of Si_2Au_4 and the corresponding structure and molecular orbitals of Si_2H_4.

which bears similarities with $Si_3H_3^+$, has been successfully synthesized.[65] Our structural search indeed showed that the lowest energy isomer for $Si_3Au_3^+$ (D_{3h}, $^1A_1$) is identical to $Si_3H_3^+$. A comparison of the valence MO's between the aromatic cyclotrisilenylium ion $Si_3H_3^+$ and the auride ion $Si_3Au_3^+$ is shown in Fig. 12. As anticipated, there is a one-to-one correspondence in bonding between $Si_3Au_3^+$ and $Si_3H_3^+$. The HOMO in both species is the π bond, which is responsible for their aromaticity. The remaining MO's are responsible for the Si–Au(H) and Si–Si σ bonding. Thus, $Si_3Au_3^+$ is a 2π aromatic molecule, analogous to the well established 2π aromatic cyclotrisilenylium ion $Si_3H_3^+$ and extending the Au–H analogy to an aromatic Si–Au cluster.

Although Au and Si do not form stable alloys, the Au/Si interface has been studied extensively due to its importance in microelectronics. It has been shown that despite the fact that Au is a very stable noble metal it is highly reactive on Si surfaces even at room temperature.[66] Several metastable Si–Au alloys, including a $SiAu_4$ phase, have been observed to form in the Si–Au interface.[67] However, the nature of the chemical interactions between Au and Si in the Si–Au interface is still not well understood.[68] The finding of the Au–H analogy, the strong Si–Au covalent bonding, and the highly stable gaseous silicon auride species are consistent with the high reactivity of Au on Si surfaces and should provide further insight into the nature of the chemical interactions in the Si/Au interfaces.

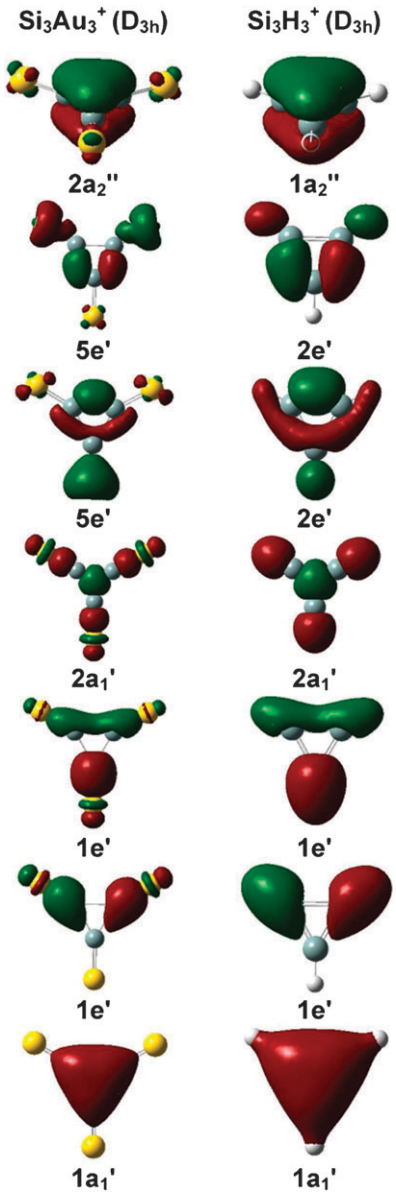

Fig. 12 Comparison of the valence molecular orbitals of $Si_3Au_3^+$ and $Si_3H_3^+$.

3.3 The Au–H analogy in B–Au alloy clusters

Because of the similar electronegativity between B and Si, it was expected that Au may also act like H in B–Au alloy clusters. We have produced and obtained preliminary PES spectra for a wide range of $B_xAu_y^-$ clusters. The first B–Au alloy cluster subjected to a detailed study was $B_7Au_2^-$,[69] because its PES spectra were relatively simple with well-resolved vibrational structures in the ground state transition at 266 nm (Fig. 13), in contrast to the complicated spectra observed for pure B_7^-, which had contributions from three isomers.[70] We hypothesized that the $B_7Au_2^-$ cluster would behave similarly as the $B_7H_2^-$ system, which is a highly stable hydride cluster with a planar C_{2v} structure.[71] Theoretical calculations showed indeed that $B_7Au_2^-$ possesses an extremely stable planar structure (Fig. 14), identical to that of $B_7H_2^-$, demonstrating that Au mimics H in its bonding to boron, analogous to the Au–Si bonding. As schematically shown in Fig. 14, the ground state structure of $B_7Au_2^-$ ($B_7H_2^-$) can be viewed as adding two Au (H) atoms to the

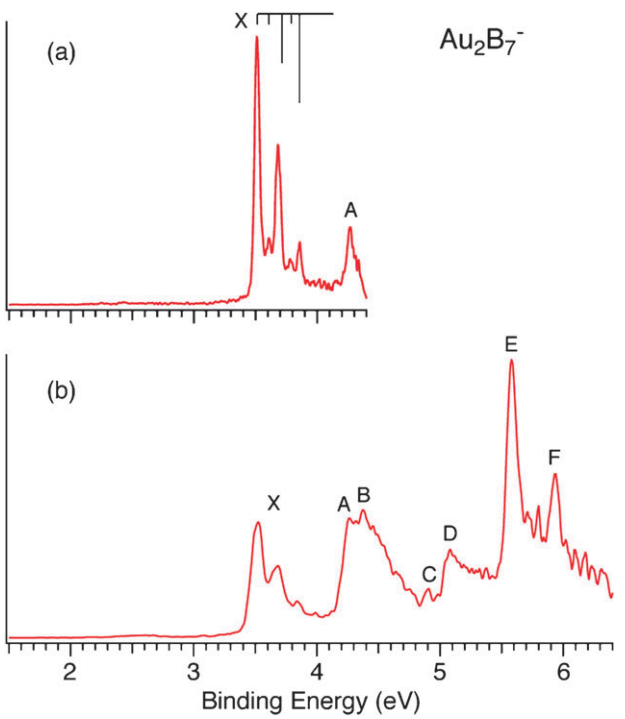

Fig. 13 Photoelectron spectra of $Au_2B_7^-$ at (a) 266 nm and (b) 193 nm.

This journal is © the Owner Societies 2010

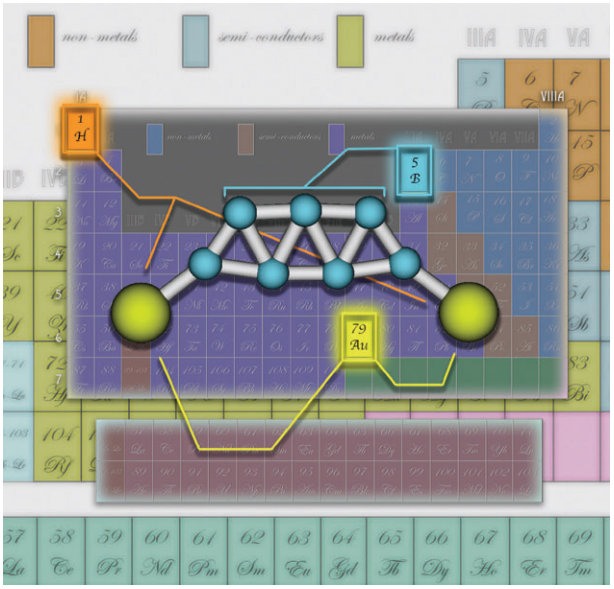

Fig. 14 Schematics showing the global minimum structure of Au_2B_7 and the Au–H analogy in Au_2B_7 and H_2B_7.

terminal B atoms of an elongated planar isomer of B_7^-. Interestingly, this C_{2v} structure of B_7^- is a higher energy isomer[70] and it is significantly stabilized by the strong bonding with H and Au.

The bonding and stability in the planar $B_7Au_2^-$ ($B_7H_2^-$) cluster were understood on the basis of the strong covalent B–Au (H) bonding and the concepts of aromaticity and antiaromaticity.[72–74] The MO pictures of $B_7Au_2^-$ are depicted in Fig. 15. Among the twenty two occupied valence MOs, ten are due to the Au 5d orbitals (HOMO-8 to HOMO-16 plus HOMO-18 (although a few of the lower-lying orbitals have significant mixing with the B_7 backbone); seven are responsible for the formation of seven 2c–2e (two center two electron) peripheral B–B bonds (HOMO-2, HOMO-4, HOMO-7; HOMO-17, and HOMO-19 to HOMO-21); two are primarily responsible for the B–Au bonding (HOMO-3 and HOMO-5); and two are π orbitals (HOMO and HOMO-6). This leaves the HOMO-1 ($9a_1$), which is a σ-orbital delocalized mainly over the five boron atoms that are not bonded to Au. Thus, $B_7Au_2^-$ is π-antiaromatic (4π delocalized electrons) and σ-aromatic (2 delocalized σ electrons) with all other MOs representing the two 2c–2e B–Au bonds and the seven 2c–2e B–B peripheral bonds. The planar $B_7Au_2^-$ structure can then be viewed as originating from the mixing of the Au 6s-5d hybrid orbitals with one of the delocalized σ orbitals in B_7^-, thus transforming the doubly antiaromatic B_7^- into a σ-aromatic but still π-antiaromatic $B_7Au_2^-$ species. Essentially, a delocalized σ orbital, forming the original σ-antiaromatic pair of orbitals, is transformed to two B–Au localized bonds, gaining major stabilization for $B_7Au_2^-$. The elongated structure of the C_{2v} B_7 framework in $B_7Au_2^-$ or $B_7H_2^-$ is a result of the π

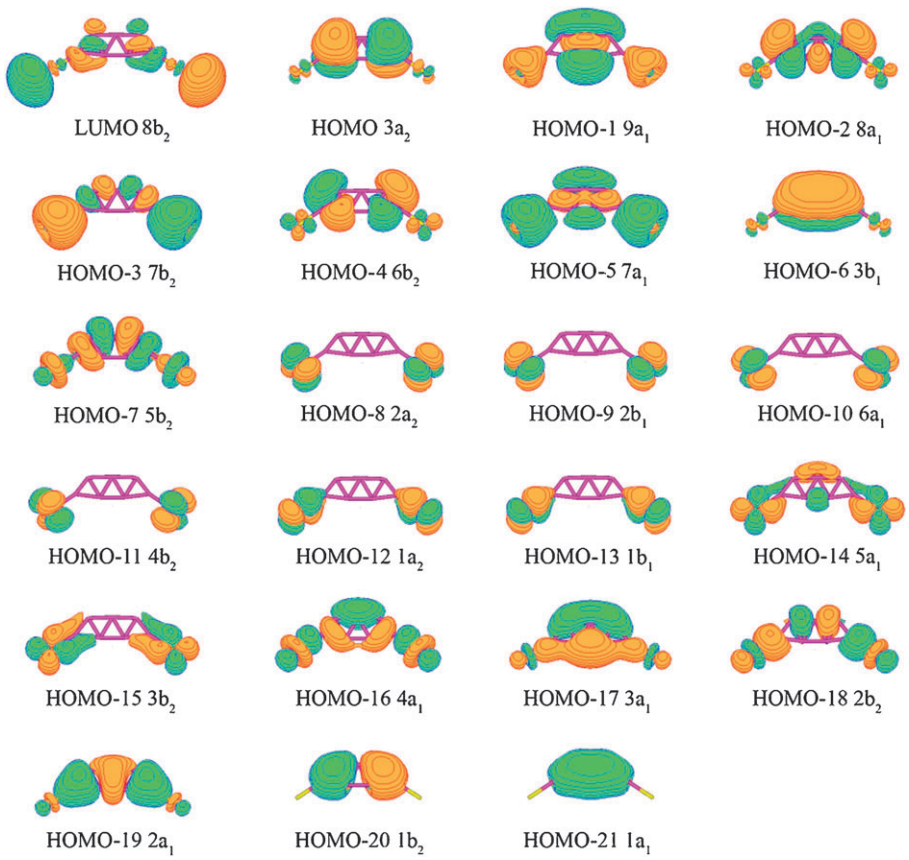

Fig. 15 Molecular orbital pictures of $Au_2B_7^-$.

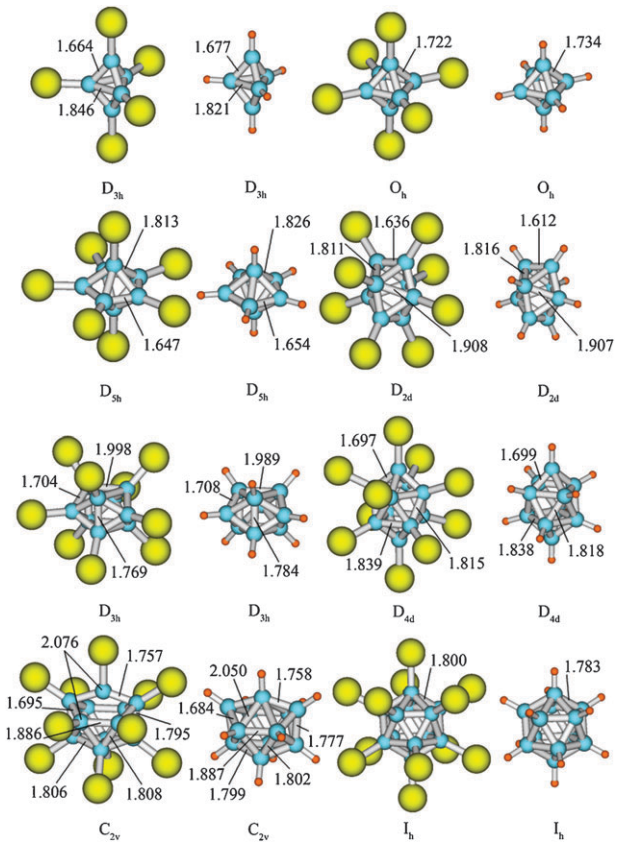

Fig. 16 Optimized geometric structures of $B_xH_x^{2-}$ and $B_xAu_x^{2-}$ (x = 5–12) (see ref. 75) with selected B–B distances in Å. (Yellow—Au; Blue—B; Orange—H)

antiaromaticity. The stability of the C_{2v} planar structure of $B_7Au_2^-$ is also reinforced by the two strong B–Au covalent bonds or B-H bonds in the case of $B_7H_2^-$.

The similarity in stability, structure, and bonding in the global minima of $B_7Au_2^-$ and $B_7H_2^-$ is analogous to the Au–H analogy in Si–Au clusters. We found that the B–Au bonds in $B_7Au_2^-$ are also highly covalent with very little charge transfer from Au to B, similar to the Si–Au bond. This finding inspired a computational investigation on the stability of closo-auro-boranes, $B_xAu_x^{2-}$ (x = 5–12),[75] which were found indeed to possess structures and bonding similar to the well-known deltahedral closo-borane cages, $B_xH_x^{2-}$, as shown in Fig. 16. The B–B bond lengths are similar between the auride and hydride boranes and the effective atomic charges on Au in $B_xAu_x^{2-}$ are also very similar to those on H in $B_xH_x^{2-}$. The results suggest that the closo-auro-borane species are new chemical compounds that may be viable for chemical syntheses in the bulk. The Au atoms in the closo-auro-boranes represent highly atomically dispersed gold and may potentially exhibit novel catalytic and chemical properties.

3.4 Covalent bonding of Au in other mixed clusters

The Au–H analogy may be a more general phenomenon and may exist in many Au-containing molecules. In a study of the Au_2H^- hydride molecule,[76] it was found that the structure of this anion cluster is linear, $[Au–Au–H]^-$, whereas the neutral cluster is triangular. The structures of this simple gold hydride are similar to the bare Au_3^- anion and its neutral, respectively. Thus, the H atom in the Au_2H hydride behaves like a Au atom!

During experiment on Au–B alloy clusters, an auro-boron oxide cluster Au_2BO^- was observed to be an intense peak dominating the Au–B mass spectra, along with weaker signals for $AuBO^-$ and Au_3BO^-. PES and computational studies showed that Au_2BO^- is a closed shell molecule with a very high electron binding energy, whereas AuBO and Au_3BO neutrals are shown to be closed shell species with large HOMO–LUMO gaps, resulting in relatively low electron affinities.[77] The structures of Au_nBO^- (n = 1–3) were compared with those of the corresponding H_nBO^- species in order to evaluate the analogy in bonding between gold and hydrogen in the new Au–BO clusters. It was found that the first gold atom does mimic hydrogen and interacts with the BO unit to produce a linear $AuBO^-$ structure with significant Au–B covalent bonding. This unit preserves its identity when interacting with additional gold atoms: a linear $Au^-[AuBO]$ complex is formed when adding one extra Au atom; two isomers are formed for $Au_2^-[AuBO]$ with close energies. The Au_nBO^- species can be alternatively viewed as Au_n interacting with a BO^- unit,[78] which contains a highly stable B≡O triple bond and has been observed as building blocks in B-rich boron oxide clusters.[79,80] Since BO^- is isoelectronic to CO, the structures and chemical bonding in Au_nBO^- can also be

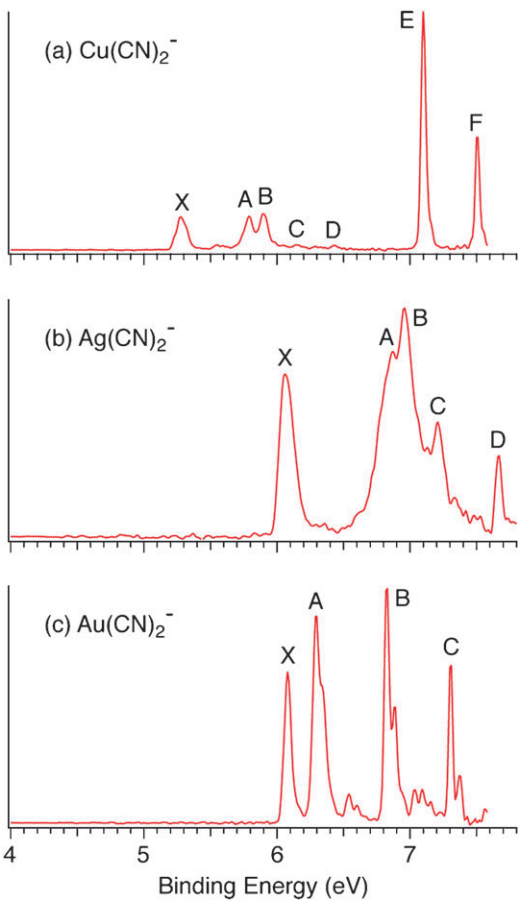

Fig. 17 Photoelectron spectra of $M(CN)_2^-$ (M = Cu, Ag, Au) at (a) 157 nm (7.866 eV).

This journal is © the Owner Societies 2010

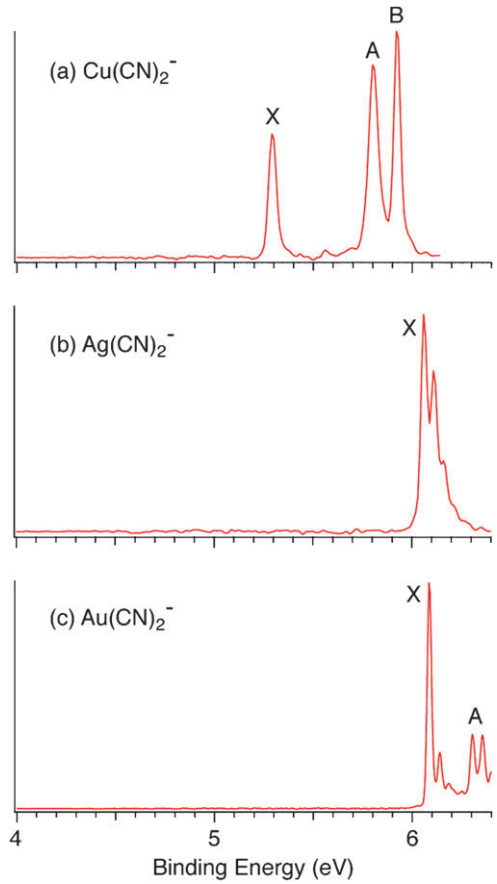

Fig. 18 Photoelectron spectra of $M(CN)_2^-$ (M = Cu, Ag, Au) at (a) 193 nm.

compared to those in the corresponding Au_nCO complexes, in which significant Au–CO bonding is observed.[81,82]

4. Evidence of significant covalent bonding in $Au(CN)_2^-$

The $Au(CN)_2^-$ ion is the most stable Au compound known for centuries, yet a detailed understanding about its chemical bonding as an isolated species was lacking until very recently.[83] Using electrospray and PES, we obtained direct experimental evidence of significant covalent characters in the Au–C bonds in $Au(CN)_2^-$ by comparison with its lighter congeners, $Ag(CN)_2^-$ and $Cu(CN)_2^-$. Vibrational progressions in the Au–C stretching mode were observed in PES spectra for all detachment transitions for $Au(CN)_2^-$ in contrast to the atomic-like transitions for $Cu(CN)_2^-$. DFT and high level *ab initio* calculations were carried out to understand the PES spectra and obtain insight into the nature of the chemical bonding in the $M(CN)_2^-$ complexes. Significant covalent characters in the Au–C bonding were shown in $Au(CN)_2^-$, consistent with the experimental observations.

Fig. 17 presents the PES spectra of $M(CN)_2^-$ (M = Cu, Ag, Au) at 157 nm. Surprisingly, there is very little similarity among the three spectra. The 157 nm spectrum of $Cu(CN)_2^-$ displays some weak signals in the lower binding energy range (X, A–D) and two sharp and intense atomic-like transitions (E, F) in the higher binding energy range. The binding energies of $Ag(CN)_2^-$ and $Au(CN)_2^-$ are significantly increased relative to those of $Cu(CN)_2^-$. The 157 nm spectrum of $Ag(CN)_2^-$ shows congested spectral features around 7 eV. Four well-resolved bands were observed for $Au(CN)_2^-$ (Fig. 17c), along with two weaker bands at around 6.5 and 7.1 eV due to multi-electron transitions.[80] Interestingly, vibrational progressions were observed in each PES band of $Au(CN)_2^-$; the X and A bands were better resolved at 193 nm, as shown in Fig. 18c. The measured vibrational frequencies were 400 cm^{-1} for the X and A bands, 480 cm^{-1} for the B band, and 520 cm^{-1} for the C band. The vibrational features should correspond to Au–C stretching according to solution phase data[84] and our calculated vibrational frequencies. In contrast, the spectrum of $Cu(CN)_2^-$ was relatively sharp even at 193 nm (Fig. 18a) without any vibrational structure. The observed vibrational progressions in the PES transitions of $Au(CN)_2^-$ suggest significant bonding interactions between Au and C, providing direct experimental evidence for the covalency in the Au–C bonding.

High-level calculations were used to optimize structures, compute electron binding energies to aid spectral assignments, and analyze the chemical bonding in $M(CN)_2^-$ (M = Cu, Ag, Au). The optimized geometries for $M(CN)_2^-$ and their respective neutrals are all linear. The computed Au–C bond length (1.99 Å) in $Au(CN)_2^-$ is significantly reduced relative to the Ag–C bond length (2.07 Å) in $Ag(CN)_2^-$ and is similar to the Au–C bond length in the monoligated AuCN (1.91 Å),[85,86] which has been suggested to possess multiple bonding characters.[87] The atomic-like PES transitions in $Cu(CN)_2^-$ are consistent with the ionic bonding nature in this system, whereas the bonding in $Ag(CN)_2^-$ should be in between.

The molecular orbital pictures for $Au(CN)_2^-$ are shown in Fig. 19. The HOMO and HOMO-8 describe strong Au–C σ bonding, whereas HOMO-6 is a strong π bonding orbital. The other valence MOs are either non-bonding or weakly bonding or antibonding. The chemical bonding in $M(CN)_2^-$ (M = Cu, Ag, Au) was also investigated using population and bond order analyses, revealing clearly less positive charge on Au and a higher Au–C bond order in $Au(CN)_2^-$ than in $Cu(CN)_2^-$ and $Ag(CN)_2^-$. Electron localization functions (ELF)[88] reflect the probability to find electron pairs, illustrating more vividly the increased covalency in the M–C bonding in $M(CN)_2^-$ from Cu to Au, as shown in Fig. 20. Fragment orbital analysis and orbital interaction analysis both reveal that the covalent character of Au–C and the remarkable stability of $Au(CN)_2^-$ stem from the strong relativistic effects of gold. The s-d hybridization significantly enhances the ability for Au to form covalent bonds with multiple bond characters. The covalent nature in the Au–C bonding gives the high stability of the $Au(CN)_2^-$ complex.

5. Conclusions

Experimental and theoretical evidence has been obtained, showing that multiple bonding exists between Au and O or S in the Au mono- and di-oxide or sulfide molecules. The Au–CN bonding in the $Au(CN)_2^-$ complex has also been found to contain strong covalent characters. In a series of

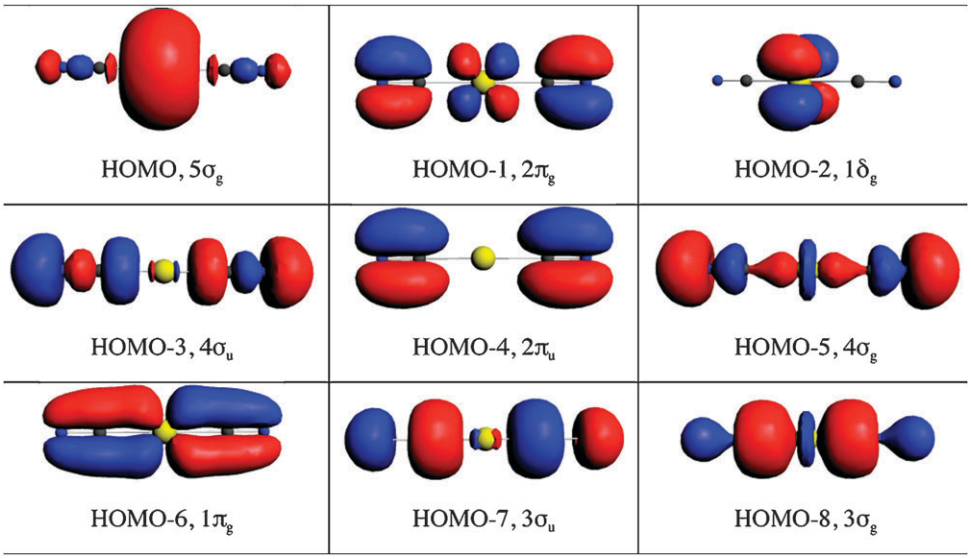

Fig. 19 Molecular orbital pictures of $Au(CN)_2^-$.

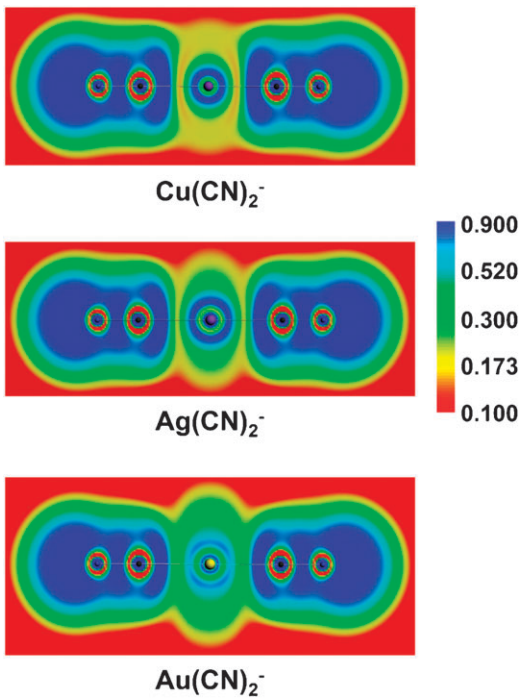

Fig. 20 Electron localization functions for $M(CN)_2^-$ (M = Cu, Ag, Au).

binary Au clusters, it has been observed that Au behaves like H to form strong covalent bonds with Si or B analogous to the respective hydrides. The covalent bonding nature of gold is at the core of ligand-protected gold nanoparticles and homogeneous catalyses of organogold. It has been increasingly recognized that the Au–S covalent bonding dictates the interfacial structures and thus the chemical and optical properties of self-assembled monolayers and ligand-protected gold nanoparticles. Gold carbene complexes have also been found to contain covalent characters, which will contribute to a better understanding of homogeneous Au catalysis. Therefore, gold, which is known to be the noblest of all metals, has been found to possess a wide range of interesting chemistry. It is conceivable that there are vast unknown chemistry and chemical compounds of Au yet to be discovered. Various multiply bonded species between Au and main group elements have been predicted and observed. Photoelectron spectroscopy in conjunction with computational chemistry is an ideal technique to probe these species and will further contribute to our understanding of the covalent nature of gold in many more compounds.

Acknowledgements

I am indebted to my theoretical collaborators, Professor Alexander I. Bolydrev from Utah State University (Logan, Utah), Professor Vlasta Bonacic-Koutecky from Humboldt University (Berlin), and Professor Jun Li from Tsinghua University (Beijing), for valuable discussions and fruitful collaborations, which constitute the bulk of this article. Support of this research by the National Science Foundation (CHE-1036387) is gratefully acknowledged.

References

1 P. Pyykkö, *Chem. Rev.*, 1988, **88**, 563–594.
2 M. C. Daniel and D. Astruc, *Chem. Rev.*, 2004, **104**, 293–346.
3 B. K. Min and C. M. Friend, *Chem. Rev.*, 2007, **107**, 2709–2724.
4 A. S. K. Hashmi, *Chem. Rev.*, 2007, **107**, 3180–3211.
5 Special issue on "Coinage Metals in Organic Synthesis", *Chem. Rev.*, 2008, **108**, issue 8.
6 P. Pyykkö, *Angew. Chem., Int. Ed.*, 2004, **43**, 4412–4456.
7 P. Pyykkö, *Inorg. Chim. Acta*, 2005, **358**, 4113–4130.
8 P. Pyykkö, *Chem. Soc. Rev.*, 2008, **37**, 1967–1997.
9 H. Schwarz, *Angew. Chem., Int. Ed.*, 2003, **42**, 4442–4454.
10 A. Bilic, J. R. Reimers and N. S. Hush, *J. Chem. Phys.*, 2005, **122**, 094708–1-15.
11 P. Maksymovych, D. C. Sorescu and J. T. Yates, *Phys. Rev. Lett.*, 2006, **97**, 146103–14.
12 M. Yu, N. Bovet, C. J. Satterley, S. Bengio, K. R. J. Lovelock, P. K. Milligan, R. G. Jones, D. P. Woodruff and V. Dhanak, *Phys. Rev. Lett.*, 2006, **97**, 166102–1-4.
13 H. Gronbeck and H. Hakkinen, *J. Phys. Chem. B*, 2007, **111**, 3325–3327.

 This journal is © the Owner Societies 2010

14 D. P. Woodruff, *Phys. Chem. Chem. Phys.*, 2008, **10**, 7211–7221.
15 T. A. Baker, C. M. Friend and E. Kaxiras, *J. Am. Chem. Soc.*, 2008, **130**, 3720–3721.
16 N. Marion and S. P. Nolan, *Chem. Soc. Rev.*, 2008, **37**, 1776–1782.
17 H. G. Raubenheimer and S. Cronje, *Chem. Soc. Rev.*, 2008, **37**, 1998–2011.
18 D. Nemcsok, K. Wichmann and G. Frenking, *Organometallics*, 2004, **23**, 3640–3646.
19 X. Hu, I. Castro-Rodriguez, K. Olson and K. Meyer, *Organometallics*, 2004, **23**, 755–764.
20 D. Benitez, N. D. Shapiro, E. Tkatchouk, Y. Wang, W. A. Goddard and F. D. Toste, *Nat. Chem.*, 2009, **1**, 482–486.
21 M. Haruta, *Catal. Today*, 1997, **36**, 153–166.
22 U. Landman, B. Yoon, C. Zhang, U. Heiz and M. Arenz, *Top. Catal.*, 2007, **44**, 145–158.
23 Special issue on "Gold: Chemistry, Materials and Catalysis", *Chem. Soc. Rev.*, 2008, **37**, issue 9.
24 F. Furche, R. Ahlrichs, P. Weis, C. Jacob, S. Gilb, T. Bierweiler and M. M. Kappes, *J. Chem. Phys.*, 2002, **117**, 6982–6990.
25 H. Hakkinen, M. Moseler and U. Landman, *Phys. Rev. Lett.*, 2002, **89**, 033401–1-4.
26 J. Li, X. Li, H. J. Zhai and L. S. Wang, *Science*, 2003, **299**, 864–867.
27 S. Bulusu, X. Li, L. S. Wang and X. C. Zeng, *Proc. Natl. Acad. Sci. U. S. A.*, 2006, **103**, 8326–8330.
28 P. Schwerdtfeger, M. Dolg, W. H. E. Schwarz, G. A. Bowmaker and P. D. W. Boyd, *J. Chem. Phys.*, 1989, **91**, 1762–1774.
29 T. Ichino, A. J. Gianola, D. H. Andrews and W. C. Lineberger, *J. Phys. Chem. A*, 2004, **108**, 11307–11313.
30 L. C. O'Brien, S. C. Hardimon and J. J. O'Brien, *J. Phys. Chem. A*, 2004, **108**, 11302–11306.
31 L. C. O'Brien, A. E. Oberlink and B. O. Roos, *J. Phys. Chem. A*, 2006, **110**, 11954–11957.
32 S. Shaji, A. Song, J. J. O'Brien, B. A. Borchert and L. C. O'Brien, *J. Mol. Spectrosc.*, 2007, **243**, 37–42.
33 Q. Sun, P. Jena, Y. D. Kim, M. Fischer and G. Gantefor, *J. Chem. Phys.*, 2004, **120**, 6510–6515.
34 D. McIntosh and G. A. Ozin, *Inorg. Chem.*, 1976, **15**, 2869–2871.
35 M. J. Griffiths and R. F. Barrow, *J. Chem. Soc., Faraday Trans. 2*, 1977, **73**, 943–951.
36 J. A. Howard, R. Sutcliffe and B. Mile, *J. Phys. Chem.*, 1984, **88**, 4351–4354.
37 P. H. Kasai and P. M. Jones, *J. Phys. Chem.*, 1986, **90**, 4239–4245.
38 X. Wang and L. Andrews, *J. Phys. Chem. A*, 2001, **105**, 5812–5822.
39 Y. Gao, W. Huang, J. Woodford, L. S. Wang and X. C. Zeng, *J. Am. Chem. Soc.*, 2009, **131**, 9484–9485.
40 W. Huang, H. J. Zhai and L. S. Wang, *J. Am. Chem. Soc.*, 2010, **132**, 4344–4351.
41 H. J. Zhai, C. Bürgel, V. Bonacic-Koutecky and L. S. Wang, *J. Am. Chem. Soc.*, 2008, **130**, 9156–9167.
42 H. Wu, S. R. Desai and L. S. Wang, *J. Phys. Chem. A*, 1997, **101**, 2103–2111.
43 P. Pyykkö, S. Riedel and M. Patzschke, *Chem.–Eur. J.*, 2005, **11**, 3511–3520.
44 M. Barysz and P. Pyykkö, *Chem. Phys. Lett.*, 1998, **285**, 398–403.
45 K. P. Hall and D. M. P. Mingos, *Prog. Inorg. Chem.*, 1984, **32**, 237–246.
46 J. W. Lauher and K. Wald, *J. Am. Chem. Soc.*, 1981, **103**, 7648–7650.
47 J. K. Burdett, O. Eisenstein and W. B. Schweizer, *Inorg. Chem.*, 1994, **33**, 3261–3268.
48 F. Scherbaum, A. Grohmann, G. Muller and H. Schmidbaur, *Angew. Chem., Int. Ed. Engl.*, 1989, **28**, 463–465.
49 A. Grohmann and H. Schmidbaur, *Nature*, 1990, **345**, 140–142.
50 B. Kiran, X. Li, H. J. Zhai, L. F. Cui and L. S. Wang, *Angew. Chem., Int. Ed.*, 2004, **43**, 2125–2129.
51 P. Pyykkö and Y. Zhao, *Chem. Phys. Lett.*, 1991, **177**, 103–106.
52 The atomization energies obtained here for the Si–H species are in good agreement with a previous study: R. S. Grev and H. F. Schaefer III, *J. Chem. Phys.*, 1992, **97**, 8389–8395.
53 X. Li, B. Kiran and L. S. Wang, *J. Phys. Chem. A*, 2005, **109**, 4366–4374.
54 B. Kiran, X. Li, H. J. Zhai and L. S. Wang, *J. Chem. Phys.*, 2006, **125**, 133204–1-7.
55 H. Lischka and H. Kohler, *J. Am. Chem. Soc.*, 1983, **105**, 6646–6649.
56 M. Bogey, H. Bolvin, C. Demuynck and J. L. Destombes, *Phys. Rev. Lett.*, 1991, **66**, 413–416.
57 R. S. Grev and H. F. Schaefer, *J. Chem. Phys.*, 1992, **97**, 7990–7998.
58 L. Andrews and X. Wang, *J. Phys. Chem. A*, 2002, **106**, 7696–7702.
59 T. Saitoh, T. Naoe and S. Ikuta, *J. Chem. Phys.*, 2005, **122**, 204314–1-11.
60 A. Korkin, M. Gluhovstev and P. v. R. Schleyer, *Int. J. Quantum Chem.*, 1993, **46**, 137–144.
61 E. D. Jemmis, G. N. Srinivas, J. Leszczynski, J. Kapp, A. A. Korkin and P. V. R. Schleyer, *J. Am. Chem. Soc.*, 1995, **117**, 11361–11362.
62 G. N. Srinivas, E. D. Jemmis, A. A. Korkin and P. v. R. Schleyer, *J. Phys. Chem. A*, 1999, **103**, 11034–11039.
63 S. P. So, *Chem. Phys. Lett.*, 1999, **313**, 587–591.
64 S. D. Li, H. L. Yu, H. S. Wu and Z. H. Jin, *J. Chem. Phys.*, 2002, **117**, 9543–9547.
65 M. Ichinohe, M. Igarashi, K. Sanuki and A. Sekiguchi, *J. Am. Chem. Soc.*, 2005, **127**, 9978–9979.
66 J. J. Yeh, J. Hwang, K. Bertness, D. J. Friedman, R. Cao and I. Lindau, *Phys. Rev. Lett.*, 1993, **70**, 3768–3771.
67 Z. Ma and L. H. Allen, *Phys. Rev. B*, 1993, **48**, 15484–15389.
68 J. Ivanco, H. Kobayashi, J. Almeida, G. Margaritondo and E. Pincik, *J. Appl. Phys.*, 2001, **90**, 345–351.
69 H. J. Zhai, L. S. Wang, D. Y. Zubarev and A. I. Boldyrev, *J. Phys. Chem. A*, 2006, **110**, 1689–1693.
70 A. N. Alexandrova, A. I. Boldyrev, H. J. Zhai and L. S. Wang, *J. Phys. Chem. A*, 2004, **108**, 3509–3517.
71 A. N. Alexandrova, E. Koyle and A. I. Boldyrev, *J. Mol. Model.*, 2006, **12**, 569–576.
72 A. I. Boldyrev and L. S. Wang, *Chem. Rev.*, 2005, **105**, 3716–3757.
73 A. N. Alexandrova, A. I. Boldyrev, H. J. Zhai and L. S. Wang, *Coord. Chem. Rev.*, 2006, **250**, 2811–2866.
74 D. Y. Zubarev, B. B. Averkiev, H. J. Zhai, L. S. Wang and A. I. Boldyrev, *Phys. Chem. Chem. Phys.*, 2008, **10**, 257–267.
75 D. Y. Zubarev, J. Li, L. S. Wang and A. I. Boldyrev, *Inorg. Chem.*, 2006, **45**, 5269–5271.
76 H. J. Zhai, B. Kiran and L. S. Wang, *J. Chem. Phys.*, 2004, **121**, 8231–8236.
77 D. Y. Zubarev, A. I. Boldyrev, J. Li, H. J. Zhai and L. S. Wang, *J. Phys. Chem. A*, 2007, **111**, 1648–1658.
78 H. J. Zhai, L. M. Wang, S. D. Li and L. S. Wang, *J. Phys. Chem. A*, 2007, **111**, 1030–1035.
79 H. J. Zhai, S. D. Li and L. S. Wang, *J. Am. Chem. Soc.*, 2007, **129**, 9254–9255.
80 S. D. Li, H. J. Zhai and L. S. Wang, *J. Am. Chem. Soc.*, 2008, **130**, 2573–2579.
81 H. J. Zhai, B. Kiran, B. Dai, J. Li and L. S. Wang, *J. Am. Chem. Soc.*, 2005, **127**, 12098–12106.
82 Y. L. Wang, H. J. Zhai L. Xu, J. Li and L. S. Wang, *J. Phys. Chem. A*, 2010, **114**, 1247–1254.
83 X. B. Wang, Y. L. Wang, J. Yang, X. P. Xing, J. Li and L. S. Wang, *J. Am. Chem. Soc.*, 2009, **131**, 16368–16370.
84 P. Schwerdtfeger, P. D. W. Boyd, A. K. Burrell and W. T. Robinson, *Inorg. Chem.*, 1990, **29**, 3593–3607.
85 O. Dietz, V. M. Rayn and G. Frenking, *Inorg. Chem.*, 2003, **42**, 4977–4984.
86 T. Okabayashi, E. Y. Okabayashi, F. Koto, T. Ishida and M. Tanimoto, *J. Am. Chem. Soc.*, 2009, **131**, 11712–11718.
87 P. Zaleski-Eigierd, M. Patzschke and P. Pyykkö, *J. Chem. Phys.*, 2008, **128**, 224303–1-5.
88 A. D. Becke and K. E. Edgecombe, *J. Chem. Phys.*, 1990, **92**, 5397–5403.